**THE GLOBAL DISTRIBUTION OF NEAR-SURFACE HYDROGEN ON MARS.** W.C. Feldman[1], T.H. Prettyman[1], W.V. Boynton[2], S.W. Squyres[3], D.L. Bish[1], R.C. Elphic[1], H.O. Funsten[1], D.J. Lawrence[1], S. Maurice[4], K.R. Moore[1], R.L. Tokar[1], D.T. Vaniman[1], [1]Los Alamos National Laboratory (Los Alamos NM 87545 USA; wfeldman@lanl.gov), [2]Lunar and Planetary Laboratory (University of Arizona, Tucson, AZ), [3]Cornell University (Ithaca, NY), [4]Observatoire, Midi-Pyrenees (Toulouse, France)

**1. Introduction:** Prime objectives of the neutron spectrometer (NS) component of the Gamma-Ray Spectrometer suite of instruments aboard Mars Odyssey are to identify the major reservoirs of hydrogen on Mars, determine their relative contributions to its total water inventory, and estimate the portion of the current inventory that is near the surface. Although more information is required than is currently available, epithermal neutron currents alone can provide a significant lower bound of hydrogen abundances on Mars.

Observations from Viking 1, Viking 2, and Mars Pathfinder positively identified two of these reservoirs. By far the largest near-surface reservoir is comprised of the two residual polar caps, which together are sufficient to cover Mars with a global ocean about 30 m deep [1, 2]. The second is contained in the atmosphere, which if deposited on the surface, would cover Mars with a thin film of water about $10^{-5}$ m deep [3]. Although negligible in comparison, the fact that an atmospheric reservoir exists shows that it can provide a conduit that couples transient reservoirs of near-surface water ice [4,5].

It has long been speculated that Mars has had, and may still retain, a far larger reservoir of water. Topographic features such as rampart craters, collapsed chaotic terrain, massive outflow channels, and valley networks provide strong support for the past existence of large bodies of surface water [6,1,7,8]. Measurements of the areal size and depth of all paleo-water and volcanic features led to an estimate of a total water inventory equivalent to a global ocean that was between 100 and 500 m thick [1]. Measurements of the D/H ratio have allowed predictions that between 5 and 50 m of this inventory was lost to space [9,10,11,12,13]. Altogether, these estimates lead to between 20 and 465 m of water from the juvenile Martian inventory that is not accounted for.

First analyses of Mars Odyssey neutron and gamma-ray data showed that reservoirs of hydrogen do indeed exist poleward of about $\pm 50^{o}$ latitude [14,15,16,17]. Mars Odyssey neutron observations also revealed a near equatorial hydrogen reservoir [15] that maximizes in Arabia Terra and its antipode. Initial quantitative estimates of hydrogen abundances in these investigations were normalized to an assumed 1% $H_2O$ content by mass for the Viking 1 landing site [18,19]. However, a recent analysis of the seasonal variation of the $CO_2$ frost cover at the north pole has allowed an independent absolute calibration of the three neutron energy bands measured using the NS aboard Mars Odyssey [20,21]. This calibration allows a reinterpretation of neutron fluxes measured globally to provide a lower bound of the hydrogen abundance within about 1 m of the Martian surface. A determination of true hydrogen abundances requires knowledge of the stratigraphy of hydrogen-bearing layers because the presence of an overlying relatively desiccated layer would mask enhanced abundances of a lower layer [20,22].

**2. $CO_2$ Frost-Free Epithermal Neutron Counting Rates:** The sensor element of the NS is a segmented cubical block of borated plastic scintillator [23,24]. This design allows measurements of upward currents of thermal (energies, E, less than 0.4 eV), epithermal (0.4 eV<E<0.7 MeV) and fast (0.7<E<2 MeV) neutrons. Absolute calibration of all three energy ranges was made using counting rates measured when the spacecraft was poleward of $+85^{o}$ N Latitude near $L_S \sim 10^{o}$, when the thickness of the $CO_2$ seasonal frost cover at the north pole was greatest [20,21].

The connection between measured counting rates and neutron energy distributions is made by combining our absolute calibration with simulations of neutron counting rates using the Monte Carlo Neutral Particle computer code, MCNPX, fitted with a special planetary boundary patch developed for Mars [21]. The relationship between the water-equivalent hydrogen content ($W_{H2O}$) of soil having the composition measured at Mars Pathfinder [25] and the calibrated counting rates (Epi) can be fit quite well (correlation coefficient, R = 0.9996) by the power law function,

$$W_{H2O} = 1.31\ [Epi]^{-1.72}. \qquad (1)$$

A $CO_2$ frost-free map of epithermal counting rates constructed from the first year of mapping data is shown in Figure 1. Correction of all counting rates for variations in cosmic rays, global variations in atmospheric thickness, and effects of variations in the NS high voltage were made by normalizing peak areas for each measured spectrum to the average counts summed over ±0.5 day when the spacecraft was equatorward of $\pm 40^{o}$ latitude [21]. Corrections were also made for variations in atmospheric thickness due to topography [21].

An overview of Figure 1 shows that Mars can be separated into three domains that have very different character. A large spatial domain north of $+50^{o}$ latitude is marked by very low epithermal neutron counting rates. The minimum rate surrounds the north pole and a secondary minimum is centered at about $-130^{o}$ east longitude between $65^{o}$ and $70^{o}$ north latitude. The

spatial domain of low counting rates is pinched off, being narrowest at about –45° East Longitude in north Acidalia. South of –50° the map is dominated by low counting rates in a broad ellipse with its long axis pointing toward 110° east longitude. At mid-latitudes between ±50°, a mixed pattern of both low and high counting rates exists, having minima within Arabia Terra and its antipode.

**3. Maps of Lower-Bound Estimates of Hydrogen on Mars:** The epithermal-neutron counting-rate map of Figure 1 was converted to lower-bound abundances of water-equivalent hydrogen using Equation 1. The result is shown in Figure 2. Two different reservoirs are evident. The component having large hydrogen abundances poleward of ±50° latitude corresponds to terrain poleward of the red-yellow wavy contour in the top panel of Figure 2. Although abundances in the south range between 20% and 50% by mass, those in the north extend to 100%. Abundances of hydrogen equatorward of these contours (the second reservoir) range between 2% and 9% by mass with a most probable value of 4%.

Inspection of Figure 2 reveals several striking observations. First, the two largest discrete reservoirs at equatorial latitudes occur at antipodal longitudes. That in Arabia Terra is centered near the equator at 25° east longitude, and its antipode is just below the equator at about 185° east longitude. Both maximize between 8% and 8.5% ± 1.3% water equivalent hydrogen, and are bisected by the zero km elevation contour. Relative maxima extending beyond these absolute maxima also follow the zero-km elevation contour. $H_2O$ weight fractions for selected mid-latitude sites are collected in Table I. Other observations worth noting are that Alba Patera at +40° latitude and 115° west longitude is a relative maximum, the terrain just beyond

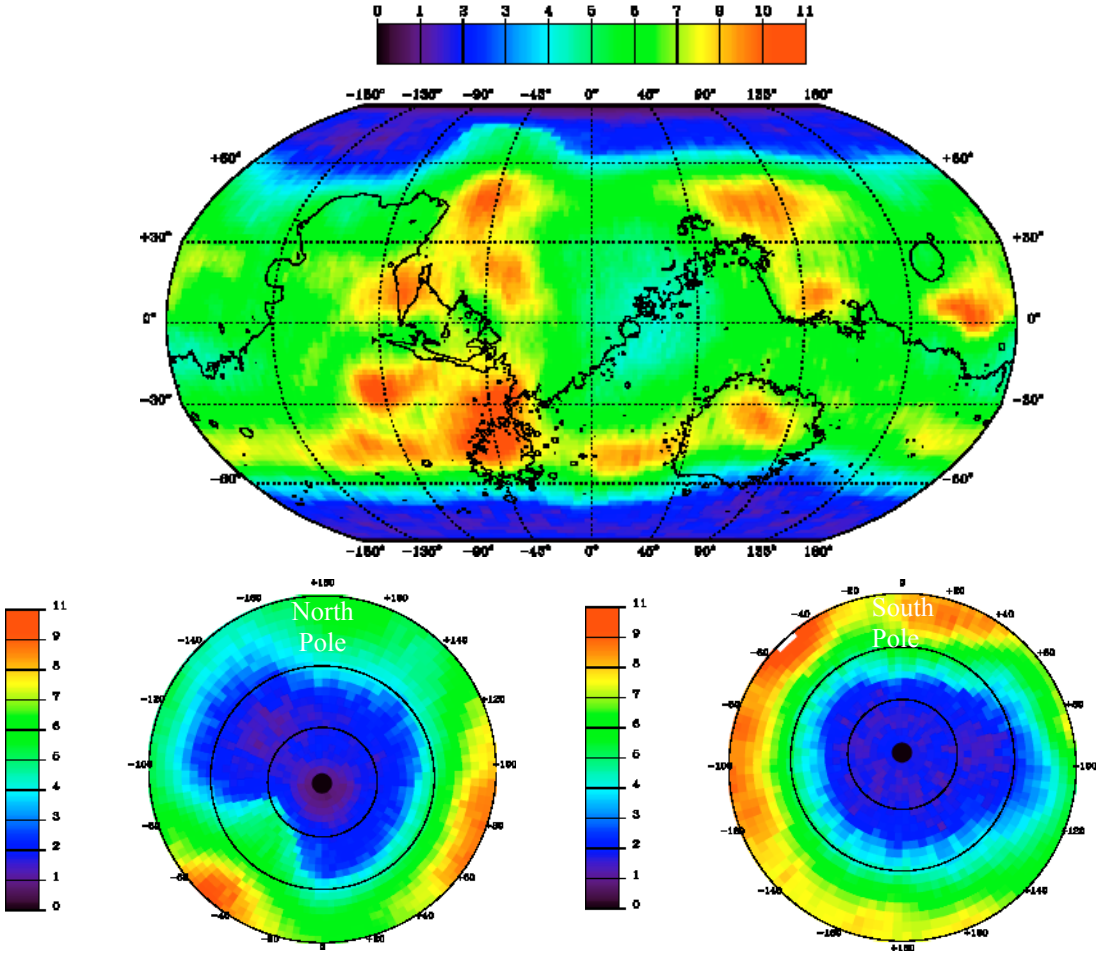


**Figure 1**. A $CO_2$ frost-free map of Mars. Data south of –50° latitude were measured during the late summer in the south, [329°<$L_s$<1.7°], and data north of +50° latitude were measured after the northern summer solstice, [100°<$L_s$<131°]. A contour of topography at 0 km is superimposed on the Robinson map.

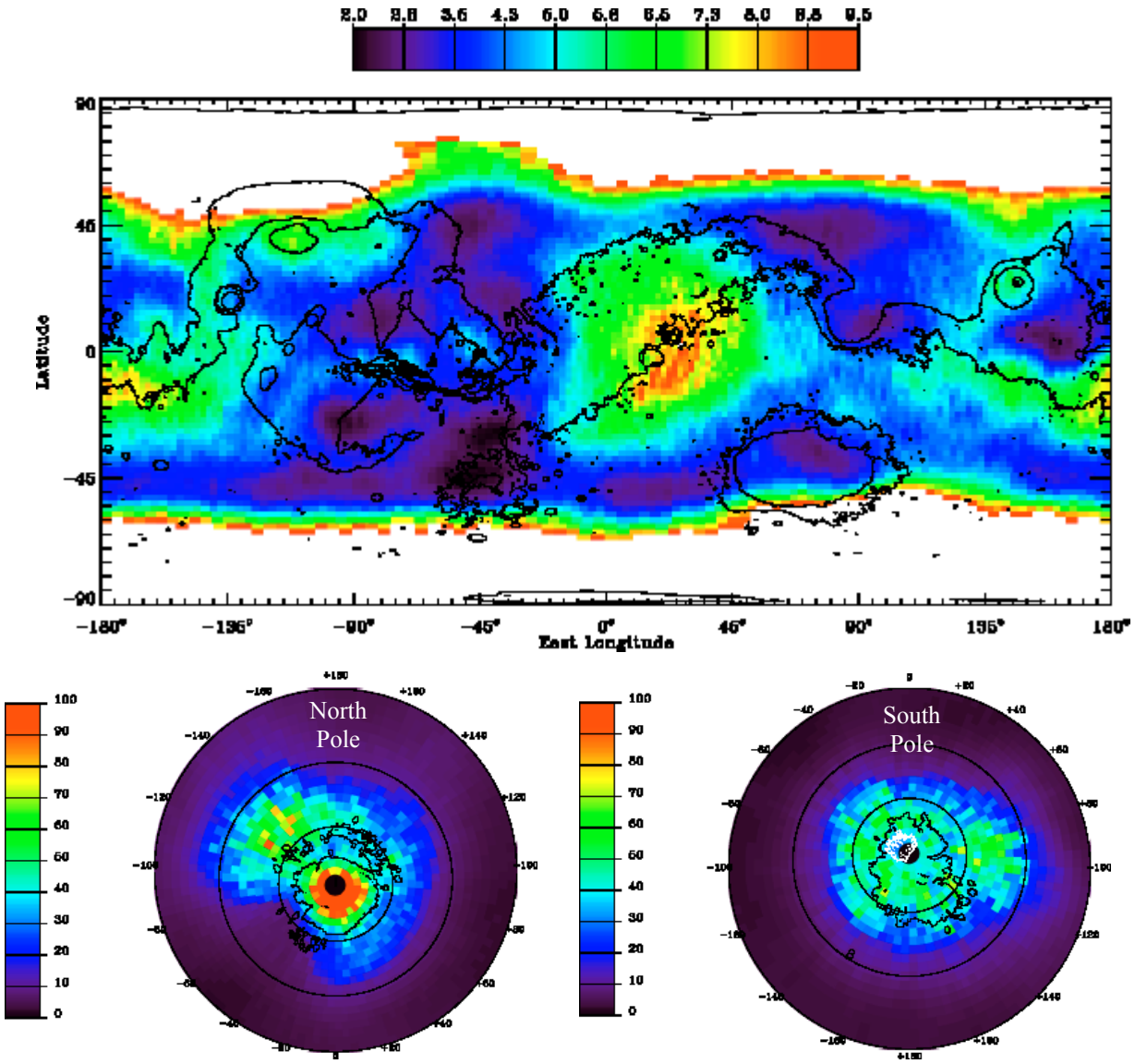


**Figure 2.** Maps of lower-bound estimates of the water abundance on Mars. The map at mid latitudes is given in cylindrical projection in the upper panel, that at latitudes poleward of ±45° are given in stereographic projection in the lower left and right hand panels, respectively. Contours of topography at the –2.5 km, 0 km, +6 km and +10 km are superimposed on the cylindrical map. Contours outlining the extent of the water-ice polar cap in the north are superimposed on the stereographic map at the lower left, and those outlining the residual cap (white line) and layered terrain (black line) in the south are shown in the lower right-hand panel.

the Kasei Valles and Valles Marineris outflow channels that debouch into Chryse Planatia have relatively low hydrogen abundance, and the relative minimum within Hellas Planitia is in its northeast sector where most global dust storms originate.

**4. Summary and Conclusions:** One year of Mars Odyssey NS epithermal-neutron data were used to construct a $CO_2$ frost-free map of Mars. These data provided input for a map of lower-bound water-equivalent hydrogen concentrations within about one meter of the Martian surface. Two major near-surface reservoirs are readily delineated. One surrounds both poles extending down to about ± 50° latitude and has relatively high-grade deposits. The near-polar mass concentrations of water-equivalent hydrogen range between 20% and 100%. A second mid-latitude reservoir maximizes at antipodal locations near the equator. Water-

equivalent mass concentrations in this reservoir range between 2% and 9%.

A minimum thickness of a global covering of water can be estimated from the lower-bound water-equivalent hydrogen maps in Figure 2. The results are tabulated in Table 2. If the thickness of these deposits is no more than the 1m nominal detection depth, then the total inventory of near-surface hydrogen amounts to about a 13-cm global layer of water. If, for example, the deposits extend to a depth of 1 km, then the inventory could amount to about a 130 m global layer. Although orbital neutron data only reflect hydrogen concentrations within about 1 m of the Martian surface, they provide no constraints on how deep the deposits may extend. If the foregoing 1 km depth estimate applies, these deposits contain an important part of the Martian inventory of juvenile water inferred from geomorphic studies [1,6,8,26].

**References:** [1] Carr, M.H. (1986) Icarus 68, 187-216. [2] Smith, D.E., et al. (1999) Science, 284,1495-1503. [3] Jakosky, B.M., C.B. Farmer (1982) J. Geophys. Res., 87, 2999-3019. [4] Jakosky, B.M., R.M. Haberle (1992), in *Mars*, Kieffer, H.H., B.M. Jakosky, C.W. Snyder, M.S. Matthews, eds., pp969-1016, U. of A. Press, Tucson. [5] Mellon, M.T., B.M. Jakosky (1993) J. Geophys. Res., 98, 3345-3364. [6] Baker, V.R. (2001) Nature, 412, 228-236. [7] Carr, M.H. (1996) *Water on Mars*, 229 pp, Oxford U. Press. [8] Jakosky, B.M., R.J. Phillips (2001) Nature, 412, 237-244. [9] Yung, Y.L. (1988) Icarus, 76, 146-159. [10] Luhman, J.G., et al. (1992) Geophys. Res. Let., 21, 2151-2154. [11] Carr, M.H. (1990) Icarus, 87, 210-227. [12] Jakosky, B.M. (1991) Icarus 94, 14-31. [13] Leshin, L.A. (2000) Geophys. Res. Lett., 27, 2017-2020. [14] Boynton, W.V., et al. (2002) Science, 297, 81-85. [15] Feldman, W.C., et al. (2002) Science, 297, 75-78. [16] Mitrofanov, I., et al. (2002) Science, 297, 78-81. [17] Tokar, R.L., et al. (2002) Geophys. Res., Lett. 29, doi:10.1029/2002GL015691.[18] Biemann, K, et al. (1977) J. Geophys. Res., 82, 4641-4658. [19] Anderson, D.M., A.R. Tice (1979) J. Mol. Evol., 14, 33-38. [20] Feldman, W.C., et al. (2003) J. Geophys. Res., Submitted. [21] Prettyman, T.H., et al., J. Geophys. Res., Submitted. [22] Feldman, W.C., et al. (1993) J. Geophys. Res., 98, 20855-20870. [23] Feldman, W.C., et al. (2002) J. Geophys. Res., 107, DOI 10.1029/2001JA000295. [24] Boynon, W.V., et al. (2003) Space Sci. Rev., Submitted. [25] Wänke, H., et al., (2001) Space Sci. Rev. 96 317-330. [26] Squyres, S.W. (1989) Icarus, 79, 229-288.

Table 1 Water-Equivalent Hydrogen for Selected Mid-Latitude Sites

| Site | (Latitude, Longitude) | Weight Fraction |
|---|---|---|
| Alba Patera | (+37.5°, -112.5°) | 6.7 ± 1.0 % |
| Arabia | (- 2.5°, +27.5°) | 8.5 ± 1.3 % |
| Arabia Antipode | (-12.5°, -177.5°) | 8.0 ± 1.2 % |
| Argyre | (-47.5°, -42.5°) | 2.3 ± 0.4 % |
| Pathfinder | (+17.5°, -32.5°) | 2.7 ± 0.4 % |
| Sinus Meridiani | (+ 2.5°, -2.5°) | 6.5 ± 1.0 % |
| Solis Planum | (- 22.5°, -92.5°) | 2.3 ± 0.4 % |
| Viking 1 | (+ 22.5°, - 47.5°) | 2.9 ± 0.4 % |
| Viking 2 | (+47.5°, +132.5°) | 5.7 ± 0.9 % |

Table 2 Equivalent Global Thickness of Water Layer

$$\rho\, D \iint W_{H2O}\, d\Omega / 4\pi$$

| Latitude Band | D = 1 m | D = $10^3$ m |
|---|---|---|
| $\Lambda > +45^\circ$ | 3.8 cm | 38 m |
| $\Lambda < -45^\circ$ | 4.4 cm | 44 m |
| $-45^\circ < \Lambda < +45^\circ$ | 5.3 cm | 53 m |
| Total | 13.4 cm | 134 m |